Studies Regarding Molding Process for Industrial Rubber Products

HORIA CIOBAN [1]*, LUCIAN BUTNAR[2], CONSTANTIN GHITA[2]

1- Technical University of Cluj-Napoca, North University Center Of Baia Mare, 62A Victor Babes Str., 430083, Baia-Mare, Romania
2- Valahia University, Carol I Bvd., 130024, Targoviste, Romania

Manufacturing process of rubber parts have to take into consideration a set of parameters of production to accomplish the requirements of the quality standards, especially in the automotive industry. Starting from input data obtained from different rubber parts production process, this paper presents results and conclusion obtained with simulation software and specific application based on numerical methods, compared with measurements obtained in industrial process. Benefits of 3D simulations lead to important product development cycle time reduction, radical manufacturing cost reduction and possibility to optimize cycle times and product quality.

Keywords: rubber injection process; Finite Element Analysis; numerical methods

Specific for rubber components in the automotive industry is series or mass production and a large diversity of sizes and shapes [5, 7]. The main process is the injection in molds that have the capability to control parameters like pressure, temperature or induction time. The bushing presented in figure 1 is a multilayer structure and it is a typical component for car suspension.

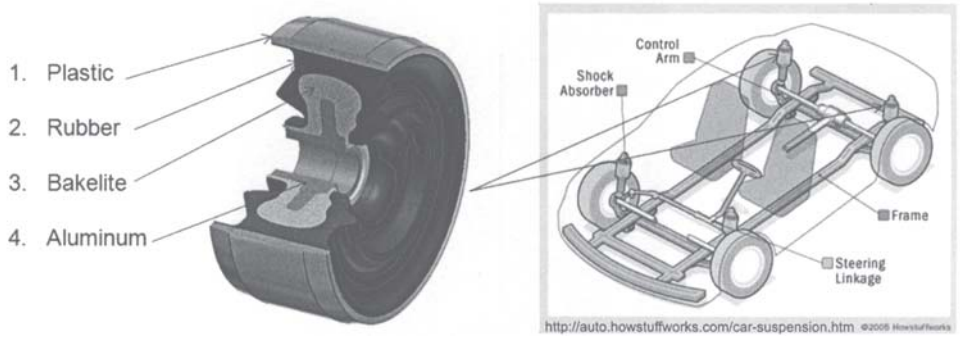

Fig..1. Bushing as a component of a car suspension

The most common defect can be detected after the injection of rubber and the bushing is pressed in an aluminum frame. Between the outer plastic ring and the rubber layer appear empty spaces (thin cavities). The vibrations coming from car's wheels generate friction between these two layers. The clients are complaining about a noise like a creak, amplified by the car chassis.

A section in the bushing shows the presence of the empty spaces between the outer ring and rubber and these are generated by a weak adherence. An important observation is also the position of the cavities, placed between the injection points.

As a consequence of all facts previously presented, thousands of bushing subassemblies are rejected from delivery and it produces hundreds thousands Euro loses / year. Looking for the possible causes, each segment of the production process can be a parameter that affects the quality of the product: raw material (different receipts for each part), spare parts coming from suppliers (inner and outer ring, bakelite, aluminum frame), press parameters and functionality, mold, heating cycle [5].

Tests and experiments

First action taken by the bushing supplier was to identify the noisy bushings and to avoid delivery to the clients. The subassemblies were 100% controlled in a stand where a vibrations source were induced simulating the movement of the wheels on road. The noisy bushings were moved in a separate container and other tests were applied to find more information about the fault causes.

A special attention was directed to verify the material properties given by rheograms. On the other side, a monitoring system was implemented in the workshop, as a support for production and troubleshooting parameters like heating element failure, time of injection variation, cycle time variations, variation of temperatures during the cycle. Different types of molds having 8, 16 and 64 cavities with 2 and 4 injection points/cavity were also tested. Better results are obtained from 8 cavity compared with 64 cavity mold and 4 injection points compared with 2 injection points.

In the laboratory, one set of experiments was directed to record the sound using a Bruel & Kjaer Sound Level Meter and to find out the frequency range and the sound level. The results indicate a maximum around the frequency of 2.5 kHz, but this kind of tests were not considered relevant enough because the measurements system reports a 2D graph of the detected sounds and it makes an average of frequencies in the time recording.

The second set has the principle to put in evidence the vibrations produced by the friction between the outer plastic

* email: horia.cioban@ubm.ro

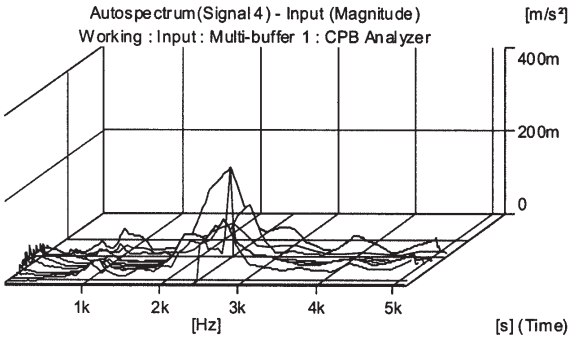

Cursor values

X = 2.44 kHz

Y = 80.3 mm/s^2

Z = 13 s

Fig. 2. Vibrometer report showing a magnitude at 2.44 kHz

ring and the rubber. The measurements were made using a Bruel & Kjaer vibrometer and four sensors were placed around the aluminum frame. After a vibration source was induced into the bushing assembly, the reports show like in figure 2, the 3D graph having *frequency* on X axis, *magnitude* on Y axis and *time* on Z axis.

Even the reply to the vibration source is different from part to part, an average of magnitude of frequencies confirms a peak around 2.5 kHz. The main advantage of this measurement system is given by online different report from each sensor.

Based on the results of these measurements, the bushings producer has the intension to automate the control process, having as a decision unit the vibrometer interface.

Mathematical Model of Solidification of Rubber

It will be studied the motion of the molten rubber into the bushing system and the heat transfer with a solidification of the material in plastic box. The molten rubber is assumed to be incompressible Newtonian fluid and the wall of the plastic box act as a thermal insulator [3].

The governing equations describing the coupled fluid flow and heat transfer with solidification are the continuity equation, the Navier-Stokes equations, the energy equation and the mushy zone equation:

$$\begin{gathered}\nabla u = 0 \text{ (incompressible fluid);}\\ \rho\left(\frac{\partial u}{\partial t}+u\nabla u\right)-\nabla\left[-pI+2\mu(\nabla u)_{sym}\right]=\rho g+F_{\sigma,i},\ i=1,2 \text{ (or } i=1,2,3,4\text{) (Navier-Stokes equations);}\\ \rho C\left(\frac{\partial T}{\partial t}+u\nabla T\right)=\nabla(k\nabla T)+Q_T \text{ (energy balance equation);}\\ \frac{\partial\phi}{\partial t}+u\nabla\phi-\partial\psi_{[-1,1]}=0 \text{ (mushy zone equation),}\end{gathered} \tag{1}$$

where u, p, T and ϕ denote respectively the velocity field, scalar pressure, temperature and the solid fraction function. Here ρ and μ are the density and viscosity coefficient of the fluid; g is the gravitational acceleration, C and k are the heat capacity and the thermal conductivity of the fluid. The solid fraction satisfies the relation $-1 \le \phi \le 1$ and when the physical properties of the two zones, solid and liquid, are different, they are discontinuous on the interface (into the mushy zone).

In order to smooth the discontinuities, the viscosity, the heat capacity and the thermal conductivity are represented in terms of a regularization of Heaviside function, as

$$\begin{aligned}\rho(\phi)&=\rho_s+(\rho_l-\rho_s)H(\phi);\\ \mu(\phi)&=\mu_s+(\mu_l-\mu_s)H(\phi);\\ C(\phi)&=C_s+(C_l-C_s)H(\phi);\\ k(\phi)&=k_s+(k_l-k_s)H(\phi),\end{aligned} \tag{2}$$

where s and l are subscripts for solid and molten rubber and $H(.)$ is given by

$$H(\phi)=\begin{cases}0, & \text{if } \phi\le-\varepsilon,\\ \frac{1}{2}\left[1+\frac{\phi}{\varepsilon}+\frac{1}{\pi}\sin\frac{\pi\phi}{\varepsilon}\right], & \text{if } |\phi|<\varepsilon\\ 1, & \text{if } \phi>\varepsilon\end{cases}, \tag{3}$$

where ε is the thickness of the interface between solid and fluid zones.

The surface tension forces $F_{\sigma,j}$, acting on the interface can be proposed as

$$F_{\sigma,i}=\sigma\kappa(\phi)\delta(\phi)\vec{n} \tag{4}$$

where σ is the surface tension coefficient, $\vec{n}$ is the unit normal on the interface, $\kappa(\phi)=-\nabla\vec{n}$ is the curvature and $\delta(\phi)$ is a regularized delta function, given by

$$\delta(\phi)=m\left|\phi^2-\alpha^2\right|, \tag{5}$$

for some $m > 0$ and $\alpha > 0$.

The second term in the right hand side of the energy equation is the heat source Q_T; it represents a phase change and it is zero everywhere except in the mushy zone, where

$$Q_T=-\rho_s\left(\frac{\partial H_l}{\partial t}+u\nabla H_l\right)(1-H(\phi)) \tag{6}$$

here H_L is the latent heat given by the formula

$$H_L=Lf(T)=\begin{cases}0, & \text{if } T\le T_s\\ L\frac{T-T_s}{T_l-T_s}, & \text{if } T_s<T<T_l\\ L, & \text{if } T>T_l\end{cases} \tag{7}$$

where L is the latent leak of the rubber liquid, $f(t)$ is the liquid fraction function, T_s and T_l are the solidification temperature and melting temperature of the rubber, respectively [2].

These equations with appropriate boundary conditions constitute an unstable system of five variables u_1, u_2, p, T and ϕ as time depending functions.

Finite element method for solidification of rubber and numerical investigation.

The governing partial differential equations of unsteady unknown functions: u_1, u_2, p, T and ϕ in a bi-dimensional domain $\Omega \subset R^2$, a section in the box following the (x, y) plane.

The domain is discretized in variable space by finite element method, which yield to the following system of nonlinear ordinary differential equations

$$M\dot{Q} + KQ = F, \quad (8)$$

where Q represents the values of the corresponding unknowns U, P, T and Φ at the nodes of the finite element mesh. The matrix M corresponds to the transient terms in the governing partial differential equations and the matrix K corresponds to the advenction and diffusion terms, depending nonlinearly on U, T and Φ.

The numerical solutions of the nonlinear discretization system with appropriate boundary conditions are then obtained using an iterative scheme, developed based on the Euler's backward scheme. It imposes the following convergent condition used in the simulation

$$\left\| Q_i^{m+1} - Q_i^m \right\| \le \eta, \quad (9)$$

where the superscripts m + 1 and m denote iterative computational step, Q_i denotes the approximation of the vector $Q = (u, p, T, \phi)$ of the i-th variable on the finite element nodes. Here $||.||$ is the Euclidian norm and η is the small positive constant [4].

The example under investigation is a circular domain with radius $r_1 = r_{int} = 9.15$ mm and $r_2 = r_{ext} = 31.25$ mm. The 3D model was obtained in a CAD application (Autodesk Inventor) and was imported to a simulation environment (Autodesk Moldflow Insight) using STL Data Exchange Format file.

This domain was discretized in the first step using triangular elements [2, 3]. The model geometry (fig. 3a) leads to a ***3D mesh*** type and the volume will be filled by tetrahedral elements in the second step, when the mesh was refined near the injection points, as in figure 3b.

Depending on the process type, simulation application enables access to material databases. The material used in these bushings belongs to the *thermoset* materials category. The recommended process in this case is *reactive molding analysis* that includes rubber injection molding [4].

The receipt for the injected rubber is imposed by the car producer and is specific for this part. For this reason, a new material was added to existing database and the physical properties had to match with the rubber used in the production process. The pre-processing stage of the analysis ends with establishing the position of the injection points and setting the process parameters like mold surface temperature (85°C), melt temperature (170°C), filling control, velocity/pressure switch-over and injection machine parameters.

The analysis log generated meanwhile the analysis process is performed reports on any inputs used, any warnings or errors encountered, and provides a summary of results generated at the end of the filling and packing phases. Some of the information reported by the analysis log is displayed in table 1.

The post-processing results are shown in several graphical representations like coloured 2D and 3D diagrams, plots, reports and animations. As example, figures 4 a and b give information regarding the fill time in 2 and 4 injections points cases. The volume is filled starting with the tetrahedrons placed near the injections points (the first 3 seconds). The last areas filled by the melt (seconds 9 to 12) are situated around a midplane between the injection points and are the same where the defects occur. This indicates a possible problem of viscosity and of solidification process.

Important information is delivered also by the freeze time chart that shows the amount of time required to reach the ejection temperature, measured from the start of the cycle. If the packing and cooling phase of the simulation are insufficient to complete the solidification of the part, then no result is assigned on those nodes as they are still molten [1, 6]. Solidification of the melt is starting at 29.5 second and ends at second 43, and the last area solidified is around the middle plane, like in the filling case. In a similar way are presented temperature at the flow front, pressure at viscosity/pressure switchover, pressure at

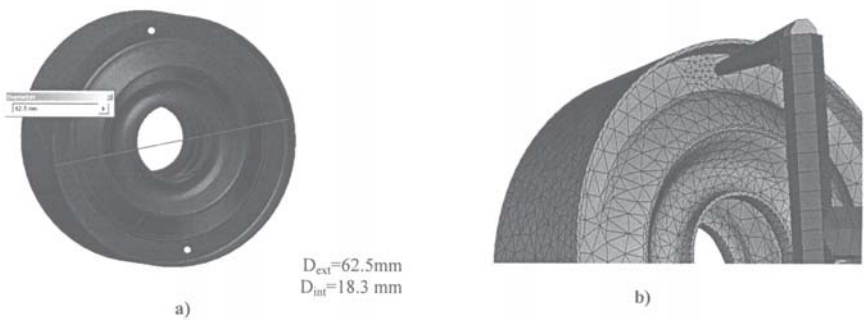

Fig..3 – a) 3D model of rubber bushing for 2 injection point; b) Refining mesh in the injection point area

Table 1
ANALYSIS RUNNING PARAMETERS

Solver	Coupled 3D	Maximum machine clamp force	7.0E+03 tonne
Solution type	Stokes	Curing time	30.00 s
Mesh Type	3D Tetrahedra	Total mass	72.9878 g
Number of tetrahedral elements	122312	Injection pressure	24.25 MPa
Total volume	52.2006 cm^3	Injection pressure at v/p switch-over	24.25 MPa
Maximum injection pressure	1.8000E+02 MPa	CPU time used	1208.80 s

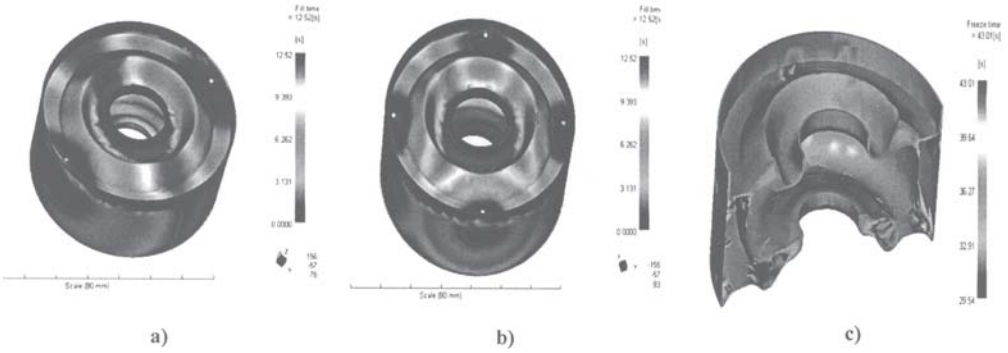

Fig..4 a) Fill time in 2 injection points case; b) Fill time in 4 injection points case; c) Freeze time

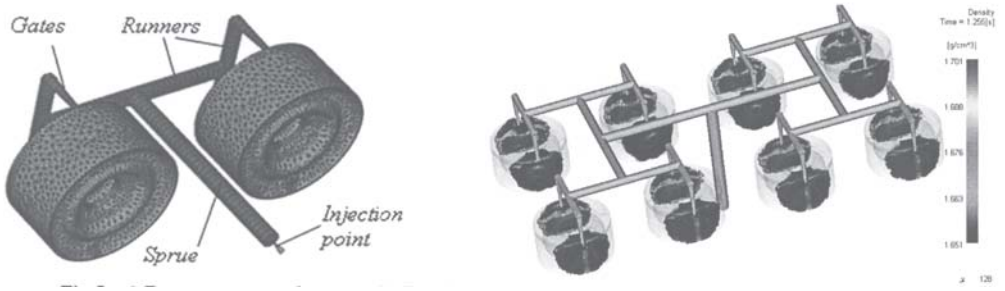

Fig..5a). Runner system elements; b) Density variation in time of the melt for 8 cavities mold

injection location, density, freeze time and other significant parameters.

The software application allows multiples studies in the same project. A second study is oriented to analyze the behavior of the melt using a two cavities mold. In this case, it has to take into consideration the running system. New elements like gates, runners and sprues were added between the injection point and the bushing model (figure 5a). The application offers the possibility to adjust the dimensions and shapes of the runner components and the meshing phase treats them like beams.

An important condition to run the analysis is the connectivity between the finite elements of the mesh. Designing the 3D model containing multiple cavities and runner system means specific operations like copying, moving or mirroring the 3D objects that can induce geometrical errors and a discontinuous mesh.

A successful analysis of the study for 2 cavity offers the possibility to open new studies for molds with 4 and 8 cavities, which is the final stage of the project because it replicates with more accuracy the real mold and process.

The density variation in time explains also how the solidification process runs. The density decreases from 1.651 g/cm^3 at second 0 to 1.701 g/cm^3 at second 43. Figure 5b presents a snapshot in second 1.256.

The typical maximum hydraulic pressure of an injection molding machine ram is around 20 MPa. When the polymer is injected and is forced into the nozzle, there is a pressure intensification factor of between 8 -15 due to the smaller area of the nozzle. The numerical results indicate also that the magnitude of the injection sources $F_{ó,i}$, $i=1,2,(3,4)$, has a considerable effect on the flow and temperature fields.

It is clearly seen that with the increasing of the injection source forces, the temperature near the injection points decrease significantly, the upper flow is too weak and at the end of the admission the temperature on the upper zone drops faster.

Using the software tool, around 200 tests were made on different configurations, changing parameters and comparing the reports. Around 100 hours/computer were performed only to run analysis. After sorting the results, the parameters having great influence in process came out.

Based on all facts observed during the simulations combined with observations from workshop and laboratories, a series of measures were taken in the production process.

First of all, special attention was paid to quality control of the raw material and those suppliers that offer better quality have been agreed.

Another important parameter that influences the process was the diameter of gates at cavity entrance. Increasing diameter with 25% reduced the fill time of the cavities. This parameter cannot be increased more because the runner system cannot be properly removed after freezing the material. A similar result is given by increasing the pressure at the injection points with 10%.

Good results were obtained by increasing the number of gates from 2 to 4 at each cavity, at 64 cavities mold. This modification has the disadvantage of high cost.

But the most significant effect was offered by an observation given by one of simulation test. It is about pressure at viscosity/pressure switchover that shows the pressure distribution through the flow path inside the mold at the switchover point. The pressure should be zero at the extremities of each flow path at the end of filling otherwise the cavity is possible to be not completely filled. The analysis shows that this parameter is influenced by the melt temperature and this led to the idea of pre-heating of all solid parts of the bushing at the same temperature as the melt.

The cumulative effects of all these changes have led to a real effect upon the quality of final product and the percentage of defects was reduced below 1%.

Conclusions

Production of rubber parts is influenced by a set of parameters and losing control of some of them has direct impact on quality of product. Simulation of the injection process is a strong and useful tool and offers a better understanding the process. Sorting the information obtained from simulations tests focuses the efforts towards the main parameters. Comparing the results of analysis offers solutions for optimizing the manufacturing. The most important impact that leads to a solution in this particular case of rubber bushing was the pre-heating of components at the same temperature as the melt.

References

1. ***, Autodesk Inc., Autodesk Moldflow Insight, User Guide, U.S.A., 2009.
2. ANGELOV, T.A., Variational and numerical approach to a steady-state rolling problem, J. Eng.Math., DOI: 10.1007/s 10665-009-9284-0
3.LIPINSKI D. M., FLENDER, E., Numerical simulation of fluid flow and heat transfer phenomena for semi-solid processing of complex casting, 5th International of Alloys and Composites, Golden, USA, 1998.
4.TIMO, T., ELASTOPLI O., Simulation applications and benefits in developing and manufacturing rubber and plastic products, Proceedings of the Sim-Serv virtual institute, pg. 2(7), vol. 2004, published at www.sim.serv.com.
5. GHITA,E., BORDEAŞU, I., CERNESCU, A., BĂLĂŞOIU, V., CIUCĂ, I., t. Plast., **47**, no.3, 2009, p.379
6. GOANTA, V., HADAR, A., ATANASOAIE, Mat. Plast., **48**, no.1, 2011, p. 71
7. CAPLAESCU, CR., MARSAVINA, L., BORDEASU, I., SEKEI, R.,Mat. Plast., **45**, no.1, 45 2008, p.97

Manuscript received: 21.05.2012

recenzie

Polimerizări ionice şi ionic - coordinative
Autor: Prof. dr. ing. Gheorghe Hubca

Lucrarea de faţă intitulată: "Polimerizări ionice şi ionic-coordinative", cu o extindere de 555 pagini, prezintă cele mai noi şi mai moderne procedee de polimerizare, care conduc la compuşi macromoleculari cu arhitectură controlată şi proprietăţi unice.

In capitolul I se realizează o comparaţie între polimerizarea radicalică şi polimerizarea ionică, scoţându-se în evidenţă caracteristicile şi avantajele proceselor ce decurg prin mecanism anionic şi cationic.

Capitolul II tratează cele mai semninificative aspecte privind polimerizarea anionică: natura monomerilor capabili să polimerizeze prin mecanism anionic, sistemele de iniţiere, mecanismul şi cinetica procesului, copolimerizarea anionică.

Capitolul III este dedicat polimerizării cu transfer de grupă, metodă ce permite obţinerea polimerilor "vii" la temperatura camerei, iar capitolul IV polimerizării cationice. Se prezintă monomerii capabili să polimerizeze prin mecanism cationic, chimismul, mecanismul şi cinetica reacţiilor de polimerizare.

Capitolul V prezintă mecanismul şi cinetica proceselor de polimerizare ce decurg prin intermediul catalizatorilor Ziegler - Natta. Se prezintă comparativ performanţele catalizatorilor Ziegler - Natta din generaţiile V şi VI cu cele ale sistemelor clasice din prima generaţie.

Capitolul VI este dedicat aspectelor legate de polimerizarea olefinelor cu catalizatori metaloceni (catalizatori Kaminski) iar capitolul VII prezintă performanţele catalizatorilor postmetaloceni.

Capitolul VIII se referă la una dintre cele mai fascinante metode de sinteză a polimerilor şi anume metateza cicloolefinelor. Se prezintă critic aspecte legate de chimismul şi cinetica reacţiei de metateză, precum şi date referitoare la copolimerizarea cicloolefinelor.

Fiecare capitol se încheie cu aplicaţii industriale ale procedeelor de sinteză prezentate.

Lucrarea, redactată la un înalt nivel ştiinţific, se adresează în principal studenţilor din facultăţile de profil, inginerilor ce urmează cursurile de master şi doctoranzilor, dar considerăm că este utilă şi specialiştilor ce lucrează în cercetare, proiectare sau producţie.

Prof. dr. ing. Mircea Teodorescu